Multimodal 3D Panoramic Imaging Using a Precise Rotating Platform

Yufu Qu, Wai L. Khoo, Edgardo Molina and Zhigang Zhu, *Senior Member, IEEE*

***Abstract*— Both panoramic and multimodal imaging are becoming more and more desirable in applications such as wide area surveillance, robotics, mapping and entertainment. In this paper, we build a precise rotating platform to generate co-registered multimodal and multiview 3D panoramic images. The platform consists of a pair of color and thermal cameras that are mounted with their optical axes pointing away from the rotation center. As a result of the precisely controlled rotation of the platform, multiview panoramic mosaics of color and thermal images can be obtained using circular perspective projection. Furthermore, the mosaics of two modalities can be precisely aligned via the analysis of their geometric relationship. In order to estimate the parameters of the cameras needed for multimodal alignment, a calibration method that is very simple to implement is proposed based on the relationship of the distance and angle of a feature point coming in and out of the field-of-view of a camera. Experimental results for multiview and multimodal alignment of stereo panoramas are given.**

I. Introduction

Panoramic imaging has been well studied, developed, and applied for capturing and understanding large field-of-view (FOV) scenes and objects. The representative examples include real-time single-lens panoramic (omnidirectional) cameras [1], [2], [3], 2D panoramic mosaics with a pure rotating camera [4], [5], stereo panoramic imaging with circular projection using one or more off-center rotating cameras [6], [7], [8], [9], [10], [11] and 3D mosaic generation with parallel-perspective projection using a translating camera [12], [13]. Panoramas captured by omnidirectional sensors have low spatial resolution which engenders low measurement accuracy and limited density of depth maps. 2D panoramic mosaics with a pure rotating camera has automatic closed-loop mosaicing, accurate moving object extraction, zoom-frame handling and multi-resolution representation capability. Stereo panoramic imaging could provide 3D panoramic images. Recently, multimodal imaging has been gaining more and more importance in applications such as surveillance, inspection and biometrics. However, the state-of-the-art is stereo panoramas with a single modality and multimodal imaging with small FOVs.

Furthermore, images that are captured with two or more separate sensor modalities, which may or may not be integrated in a single package, are not geometrically aligned, therefore posing a problem in object detection and recognition [14], [15], [16], [17], [18]. There are a few exceptions that provide perfectly geo-registered bi-modal sensors, e.g. Electro-Optical (EO) and Infrared (IR), at the optical level, but the sensors are quite limited in FOV and are also expensive [17]. Therefore, combining the advantages of both panoramic and multimodal imaging is greatly needed. It is desirable that the combinations satisfy the following two properties:

1) Multimodal images are geometrically aligned.
2) The implementation of such image devices is rather practical and inexpensive.

In this paper, we design an intelligent imaging system using a precisely controlled rotation platform with a pair of color and thermal cameras to generate co-registered multimodal images that provide a panoramic field of view, multiple viewing angles, and 3D imaging capabilities. The design uses commercial-of-the-shelf (COTS) sensors in a practical setup to satisfy the two properties listed above. Our approach can be applied to wide area surveillance, multimodal scene modeling, 3D mapping, moving target detection, security inspection and in particular, any application that requires multimodal alignment. The aligned multimodal, multi-view panoramas can be used as a background model for detecting targets using motion, 3D, thermal signatures, or a combination of these features.

The organization of the paper is as follows, Section II introduces the platform setup and control. Section III describes the calibration method for our multimodal panoramic 3D imaging. In Section IV, our approach to multimodal panoramic alignment is presented. Section V presents some experimental results. Finally, we conclude and discuss our work in Section VI.

II. Platform Setup and Control

The schematic setup of the system is shown in Fig. 1. It consists of a rotating platform, an electro-optical (EO) color camera, an infrared (IR) thermal camera and a personal computer (PC).

The rotation platform from Newport includes a rotation stage URS150BCC and a controller SMC100CC. The stage uses a DC motor that allows for rotation speeds up to $80°/s$ and features an ultra-high resolution 8,000 cts/rev rotary encoder with index pulse for precision homing. For the tightest position control, the rotary encoder is mounted directly on the worm screw. This eliminates most of the possible error sources associated with indirect read feedback devices. The controller is a single axis motion controller for DC servo motors up to 48 VDC at 1.5 A rms, with

This work is supported in part by AFOSR under Award #FA9550-08-1-0199, ARO DURIP under Award #W911NF-08-1-0531, DARPA (via DCM) under Award #W31P4Q-09-C-0459, and by NSF under grant #CNS-0551598.

Y. Qu, W. Khoo, E. Molina and Z. Zhu are with the Department of Computer Science, The City College of New York - CUNY, New York, NY 10031, USA {qu, khoo, molina, zhu}@cs.ccny.cuny.edu

W. Khoo, E. Molina and Z. Zhu are also with the Department of Computer Science, The CUNY Graduate Center, New York, NY 10016, USA

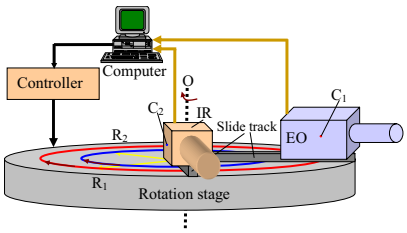

Fig. 1. Setup of the platform

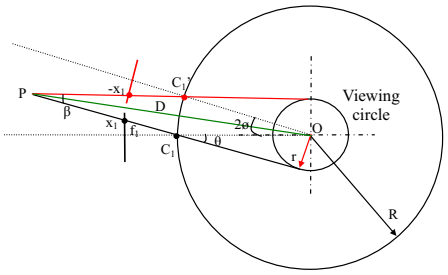

Fig. 2. Illustration of panoramic stereo pairs

an integrated RS-232-C interface for communication. The PC sends commands to the platform via the controller, such as setting and getting the velocity, position and acceleration. Consequently, the platform provides precise 360° continuous motion with a minimum incremental motion of 0.002°. The EO color camera from Sony has a 720×480 pixel resolution, with a focal length range from 6mm to 72mm, a shutter speed range from 1/60 sec to 1/10,000 sec and an IEEE-1394 firewire video output. The IR camera from FLIR can detect temperature differences as small as 0.08° in a range from $-40°$ to $+500°$C, which can be digitally resampled to generate 640×480 pixel images at a refresh rate of 50/60 Hz via an IEEE-1394 firewire output.

Two slide tracks are placed on top of the rotation platform, one of their endpoints is the platform rotation center, the other is fixed on the edge of the platform. Referring to the schematic of Fig. 1, the EO and IR cameras are mounted on top of the two slide tracks, respectively, and are looking outward from the rotation center (O). Due to physical limitations, the EO and IR cameras' two slide tracks are placed apart with an angle α. So the paths of the cameras' optical centers are two co-centric circles (C_1 and C_2) whose radii are R_1 and R_2. Each camera can also be precisely moved along the slide track so that the radius R_i can be adjusted (i.e. to have $R_1 = R_2$).

In order to build up EO/IR co-registered multi-view panoramic mosaics, the computer controls the platform to continually rotate with a constant speed, while the two cameras are continuously capturing images covering a 360° FOV, thus obtaining two image sequences. The multimodal, multiview panoramic imaging is mainly used to build a background model of static scenes for later target detection using motion, 3D, and thermal signatures. Here we want to emphasize two important points. First, we can achieve real-time processing by only using/storing the image columns of interest to build the panoramas for the background model. Second, in target detection applications, where there are moving objects, current images will be registered and compared with the background model to detect any motion, 3D, and thermal changes. The second task is beyond the scope of this paper. Here we will focus on background modeling and the calibration methods that facilitate the modeling process.

III. Stereo Panoramas and Calibration

Before we introduce our multimodal alignment technique, we will explore some of the major features of stereo panoramas under circular projection [10], [12]. Circular-perspective projection panoramas can be generated for a camera that is placed on a rotating platform. Such panoramas provide a 360° FOV of an area, and when setup appropriately, it will also produce stereo panoramas that allow 3D viewing and recovery of a scene. First, we will introduce the method of stereo panorama reconstruction. After that, we will propose a calibration method for the platform.

A. Stereo Panoramas

In Fig. 2 we have a top-down view of a camera at location C_1, looking away from and rotating around the axis O. The camera moves along the circle with radius R. If we consider a column in the cameras image plane that is to the right (or left) of the center column, as the camera moves, it will create a panorama projection onto a cylinder with radius r, which is illustrated as a "viewing circle" in Fig. 2. The viewing angle rays of these panoramas will be tangent to the projection cylinders that they generate and will cross the circle of the cameras path.

Note that for forward and backward viewing angles, the projection cylinders will have the same radius, but the panoramas will be different since they are generated from two opposite directions. We use this to generate a pair of stereo mosaics from the EO camera (or the IR camera), by choosing a pair of symmetric non-central slits (columns in the image plane) with an angle 2θ between the slits. In this symmetric stereo configuration, the epipolar lines are horizontal lines. The depth D of a 3D point P can be represented as:

$$D = \frac{r}{\sin(\frac{\beta}{2})} \tag{1}$$

where r is the radius of the viewing circle, and $\beta = 2\theta - 2\phi$ is the angular *disparity* of a pair of corresponding points in the two stereo mosaics, which correspond to the 3D point P as it is viewed by the camera at two different locations C_1 and C_1' with an angular distance of 2ϕ . The angle θ is a fixed angle for the given circular path R and viewing circle r, given by the relation $\sin\theta = r/R$. To calculate the angle 2ϕ, we have to find corresponding points in the two stereo mosaics. Assume the pixel shift between the corresponding points in the horizontal axis u of the two panoramic images is du, then $2\phi = du \times (s/n)$, where s is the rotation velocity (degree/second) of the platform and n is the image capture rate (pixel/second) of the camera.

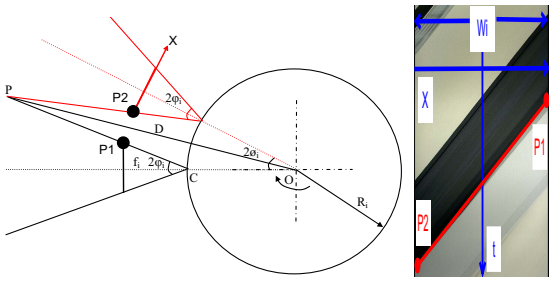

(a) Top view (b) CEPI

Fig. 3. Illustration of calibration

B. Calibration

We take advantage of the accurately controlled rotating platform to calibrate each camera. We first describe the basic principle, then we will present our approach using epipolar plane images (EPIs) [19]. As seen in Fig. 3, we assume the field of view of the camera is $2\varphi_i$ ($i = 1, 2$, 1 for EO and 2 for IR). The camera must rotate an angle of $2\phi_i$ ($i = 1, 2$) for a feature point P to first come into the field of view of the camera at P_1 in the image and then go out of the FOV of the camera at P_2 in the image (Fig. 3(a)). D is the distance of a point P from the rotation center O of the platform. In triangle $\triangle$POC, using the basic law of sines for triangles, we have:

$$\frac{D}{\sin(180^\circ - \varphi_i)} = \frac{R_i}{\sin(\varphi_i - \phi_i)} \ (i = 1, 2) \qquad (2)$$

In (2), D is measured in the calibration step; ϕ_i can be calculated from a camera's central EPI (CEPI) as discussed below. The rotation radius R_i and the angle φ_i (which is half of the FOV) are the two unknown parameters. In order to obtain the rotation radius R_i, we have to use at least two feature points (e.g. P_a and P_b), with known distances $D = D_a$ and $D = D_b$, and the rotating angles $\phi_i = \phi_{ia}$ and $\phi_i = \phi_{ib}$, respectively. We now have $D_a \sin(\varphi_i - \phi_{ia}) = D_b \sin(\varphi_i - \phi_{ib})$ $(i = 1, 2)$, which we can use to calculate φ_i. And then using (2), we can solve for R_i

$$R_i = D\frac{\sin(\varphi_i - \phi_i)}{\sin(\varphi_i)} \qquad (3)$$

After we obtain φ_i and since we know the image width is W_i, we can calculate the focal length f_i

$$f_i = \frac{W_i}{2\tan(\varphi_i)} \qquad (4)$$

Our approach to calculating ϕ_i is to generate a central epipolar plane image (CEPI) for each camera, which is done by simply taking the central row from each image in a camera's sequence and stack them up (Fig. 3(b)). In theory, we only need to find, in the CEPI, the vertical locations (i.e., times) a feature point P entered and exited the FOV of the camera to calculate ϕ. However, in order to improve the accuracy we use the following method to calculate ϕ. According to Li, and et al [8], the loci of a feature point in the CEPI are approximately a straight line. That is to say, the relation between ϕ and x coordinate of image is approximately linear. So we can extract all edge points in the loci of the point P and fit them, and obtain the slope K of the loci line. Finally, $2\phi_i = K \times W_i \times \frac{s}{n}$, where W_i is the image width. s and n are defined in Section III-A.

Fig. 4. Central PVI alignment from EO and IR image sequences

IV. Multimodal Panoramic Alignment

We will first discuss the simplest case of multimodal panoramic alignment: the alignment of the central panoramic view images (CPVIs), taken from both central columns of the EO and IR cameras, resulting in panoramic mosaics with a viewing circle of radius 0. This includes the horizontal and vertical alignments. Then we will discuss further processing requirements in aligning panoramic images coming from the non-central columns in order to generate multimodal stereo panoramas. To enable the complete alignment of two modalities, all the information we need comes from the spatial-temporal images from each modality, the CPVI composed of the central columns of the frames of the sequence, and the CEPI composed of the central rows of the frames of the sequence, when the platform undertakes a rotation with constant speed. In this section, we describe the details of the alignment mechanism using these two kinds of images. We assume all the camera parameters needed in the alignment, namely R_1, R_2, f_1, and f_2 have been found using the method in Section III.

A. Central panoramic view image alignment

First, we need to obtain the value of the angle α between the two cameras. To accomplish this, we generate two central panoramic view images (CPVI) using only the single central column of each EO and IR image, respectively. We then select (manually or automatically) a few pairs of corresponding feature points in the CPVIs of the EO and IR cameras (Fig. 4), and calculate the offsets in the horizontal direction for the matching feature points. Finally, we calculate the average value of these offsets $d\overline{\alpha}$, then we can align the EO and IR panoramas in the horizontal direction by shifting the IR image $d\overline{\alpha}$ pixels. This also gives us the angle α:

$$\alpha = d\overline{\alpha} \times \frac{s}{n} \qquad (5)$$

between the two cameras.

Due to the cameras different positions from the platform center, FOVs, and image resolutions, we also need to align the views of the two cameras vertically (Fig. 5). Fortunately, after the horizontal alignment, we have found the column correspondences between two corresponding panoramas (EO

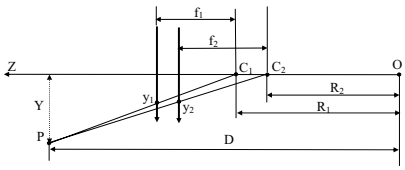

Fig. 5. The geometry of vertical alignment (side view of platform)

and IR), therefore for vertical alignment, we can work column by column.

In Fig. 5, if $R_1 = R_2$ (i.e. C_1 and C_2 are on the same circle), we can use the following equation to align the y coordinates of two corresponding points (y_1 and y_2) in the EO and IR panoramas (i.e. to map y_2 to y_2'):

$$y_2' = y_1 = \frac{f_{y1}}{f_{y2}} y_2 \tag{6}$$

where f_{y1} is the focal length of the EO camera in the vertical direction and f_{y2} is the focal length of the IR camera in the vertical direction. Since the pixel size of two cameras can differ and are not necessarily square, the focal length in the vertical direction of two cameras may not be the same as it is in the horizontal direction. So the ratio between f_{y1} and f_{y2} cannot be obtained from the ratio of focal lengths in horizontal direction as calibrated in Section III-B. However, we can obtain the ratio by comparing the height of the two images of a few objects in the CVPI when $R_1 = R_2$. Then, accurate alignment between two cameras panoramas in the vertical direction can be achieved by simple scaling. However, in reality, we may not have $R_1 = R_2$. Therefore, using (6) to align two cameras' views in the vertical direction will introduce an error. As shown in Fig. 5, the y coordinate of the corresponding points (y_1 and y_2) in the two panoramas should have the following relation, when $R_1 \neq R_2$ (i.e. to map y_2 to y_2''):

$$y_2'' = y_1 = \frac{f_{y1}}{f_{y2}} \frac{D - R_2}{D - R_1} y_2 \tag{7}$$

where D is the distance of the point P in 3D.

When we use (6) to align the second view to the first view as if C_2 was at C_1, y_2 will be mapped to y_2', which is not the same as y_2''. So the error e_y can be represented as

$$e_y = y_2' - y_2'' = \frac{f_{y1}}{f_{y2}} \frac{R_2 - R_1}{D - R_1} y_2 \tag{8}$$

In this case, we use a mechanical adjustment approach to adjust the radius of one of the cameras (along its optical axis on its slide track, see Fig. 1) so that $R_1 = R_2$.

B. Alignment of different view slits

In addition to aligning the central slits of the EO and IR cameras, we also want to align the off-center view slits in order to generate multimodal aligned stereo mosaics and obtain depth information from scenes. To generate EO-IR aligned panoramas with a viewing circle $r > 0$, we also need to align them both horizontally and vertically. The vertical alignment procedure is similar to the one for the central

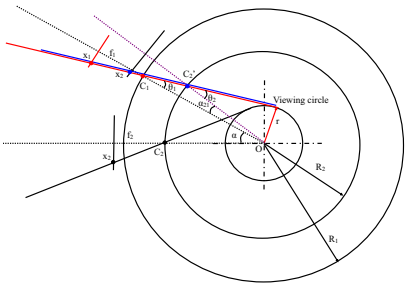

Fig. 6. Multimodal panoramic alignment

Fig. 7. Physical setup

panoramas with a viewing circle $r = 0$, after the horizontal alignment. So here we will concentrate on the horizontal alignment (this is necessary since the two sensors may have different FOVs and image resolutions). For this purpose, we need to find a pair of corresponding image columns (x_1 and x_2) in the two cameras that contributes to a pair of multimodal panoramas sharing the same viewing circle, thus aligned (Fig. 6). The requirement is that both rays from the cameras' centers C_1 and C_2 to the points x_1 and x_2, i.e. C_1x_1 and C_2x_2, have to be tangent to the same "viewing circle" whose radius is r. To align ray C_2x_2 to ray C_1x_1, we further need to align a horizontal angle $\alpha + \alpha_{21}$, where α is the global angular offset of the two cameras that we previously found in (5), and α_{21} is an additional offset angle to align two cameras at columns x_1 and x_2; it is represented as $\alpha_{21} = \theta_2 - \theta_1$, where $\tan\theta_i = x_i/f_i$, (i=1 for EO, 2 for IR); θ_1 is the incident angle between the light ray and the optical axis of EO and θ_2 is the same in IR. After this process, when C_2 is at location $C_2' = C_2^{\alpha+\alpha_{21}}$, the ray $C_2'x_2$ will be exactly the same as C_1x_1 at the correct location.

Given column x_2 in the IR camera, we can obtain the corresponding column x_1 in EO and the additional angle α_{21}:

$$x_1 = \frac{f_1}{f_2} \frac{R_2}{R_1} x_2 \tag{9}$$

$$\alpha_{21} = \arctan(\frac{x_2}{f_2}) - \arctan(\frac{R_2}{R_1} \frac{x_2}{f_2}) \tag{10}$$

For the above, we need R_1, R_2, f_1 and f_2, which have been estimated using the calibration method described in Section III-B.

V. Experimental Results

Our experiment setup is shown in Fig. 7. To perform calibration and multimodal alignment, two image sequences

(one EO and one IR) were captured when the rotating platform rotated at a constant speed. For each camera, 3600 images were taken, of size 720×480 for EO and 640×480 for IR. To show the basic principle of the alignment, only one column per image is extracted to generate a central panoramic view image. Therefore, the original resolutions of the CPVIs are 3600×480 for EO and 3600×480 for IR. However, in practice, we can use more than one column from each image, if the rotation of the platform is fast. Note that to calculate the parameters for multimodal alignment, we only need to save the CPVIs and CEPIs of the two modalities.

For the horizontal alignment, we measured 10 pairs of feature points on the EO and IR CPVIs, matched them and found their offset, which gives an average offset of $61.9°$ with a variance of $0.057°$. To find the other camera parameters (the FOV $2\varphi_i$, focal length f_i and radius R_i $i = 1, 2$), we ran the calibration approach in Section III-B.

Table I shows the calibration results of our experimental EO and IR camera system. Note that the radii and the focal lengths of the two cameras are quite different in the initial setup. After we solve for the rotation radii (R_1 and R_2) of the two cameras, we mechanically adjust the setup of the cameras such that the two rotation radii are the same, i.e., $R_1 = R_2$. After the adjustment, the platform is re-calibrated, and the result is also shown in Table I. It can be seen that $R_1 \approx R_2$ and focal lengths and FOVs are consistent before and after adjustment.

Without adjustment of the rotation radii of R_1 and R_2, there will be a vertical alignment error in the aligned images. According to (8) and current calibration results (Table I) before adjustment, the vertical alignment error is 5.89 pixels when $y_2 = 200$ and distance D is 2m; and the error is 1.09 pixels when $y_2 = 200$ and distance D is 10m. The vertical error is proportional to the ratio of the focal lengths of the two cameras and the y coordinate of the image in vertical direction, and inversely proportional to the depth of the distance D. The further the point of a 3D object is, the smaller the vertical alignment error is. After adjustment, the vertical alignment error should be zero.

For multimodal alignment, we use (9) - (10) to calculate the horizontal alignment parameters for EO and IR mosaics (Table II). In the table, we use the corresponding x locations (x_1 and x_2) in EO and IR to generate co-registered panoramas. Table II also shows the radius of each corresponding viewing circle (r) and the additional angular shift α_{21}. From Table II, we can see that the four parameters x_1, x_2, α_{21} and r are symmetric in the two opposite directions of the x axis. We also note that the angular shifts α_{21} between two cameras for different viewing circles r are slightly different. Before alignment, there is about $1.4°$ angular shift from slit to slit. After adjustment, the angular shift is very small (this should be zero if R_1 is exactly the same as R_2). Fig. 8 shows the alignment results of 3 corresponding views (-4, 0, 4), before and after platform adjustment. In the figure, the IR panoramas replaced the red channels of the EO panoramas in their overlapping regions. Before the radius adjustment, the EO and IR panoramas are aligned in the horizontal direction for all the views, but there are vertical misalignment, as shown in the right-hand close-up regions for the top edge of the LCD screen. After the radius adjustment, the EO and IR panoramas are accurately aligned in both the horizontal and vertical directions.

Multimodal alignment provides the best from two modalities; the spatial resolution shapes in EO and the unique thermal signatures in IR. For example, the warm regions can be easily detected (e.g. screen, human, etc). When perfectly aligned, it greatly facilitates target identification and visualization. To show the multimodal, multiview and stereo capabilities of our system, a video demo can be viewed in [20], generated by our mosaic based multimodal stereo rendering program, taking EO and IR panoramas as input.

VI. Conclusions and Discussions

We have designed a precise rotating platform to generate co-registered multimodal images with a panoramic field of view, multiple viewing angles and stereo images. The platform has minimum setup requirements, just needing EO and IR cameras fixed on a precise rotating platform that rotates with a constant speed around the vertical axis and the optical axes of the two cameras point away from the rotating center. The main contributions of this paper are the following. First, multimodal, multiview and stereo panoramas can be generated and accurately aligned from a practical and inexpensive platform. Second, a simple calibration method is proposed, which only requires two scene points with measured distances, to find the rotation radii and the focal lengths of two cameras. With this piece of information, the color and thermal images can be aligned on multi-view panoramic mosaics. The co-registered panoramic mosaics can be used as a background model for 3D reconstruction, multimodal object detection, and motion detection. For example, by comparing a current image with the background model, the changes in 3D, thermal, and motion can be easily detected.

In addition, the platform is not limited to using EO and IR cameras, it can be modified to include other modalities such as gamma-ray, x-ray and hyperspectral imaging. The motion of the platform is not limited to rotation as well, it also can be changed to translation to genereate multimodal, multiview and stereo panoramas.

References

[1] S. Baker and S. K. Nayar, "A theory of single-viewpoint catadioptric image formation," *IJCV*, pp. 1–22, 1999.

[2] M. Saedan, C. W. Lim, and M. H. Ang, "Appearance-based SLAM with map loop closing using an omnidirectional camera," *IEEE/ASME Int. Conf. Adv. Intell. Mechatron*, pp. 1–6, 2007.

[3] J. Meguro, T. Murata, H. Nishimura, Y. Amano, T. Hasizume, and J. Takiguchi, "Development of positioning technique using omnidirectional ir camera and aerial survey data," *IEEE/ASME Int. Conf. Adv. Intell. Mechatron*, pp. 1–6, 2007.

[4] A. Krishman and N. Ahuja, "Panoramic image acquisition," *IEEE Conf. CVPR*, pp. 379–384, 1996.

[5] Z. Zhu, G. Xu, E. Riseman, and A. Hanson, "Fast construction of dynamic and multi-resolution 360 degree panoramas from video sequences," *Image and Vision Computing*, vol. 24, pp. 13–26, 2006.

[6] J. Civera, A. J. Davison, J. A. Magallon, and J. M. M. Montiel, "Drift-free real-time sequential mosaicing," *IJCV*, pp. 128–137, 2009.

TABLE I

CALIBRATION RESULT

	Before adjustment			After adjustment		
	$2\varphi(^\circ)$	R(mm)	f(pixel)	$2\varphi(^\circ)$	R(mm)	f(pixel)
EO	44.61	192.39	877.64	44.80	286.25	873.42
IR	23.21	286.50	1551.32	23.21	286.50	1551.32

TABLE II

HORIZONTAL ALIGNMENT DATA OF MULTI-VIEW PANORAMAS ($\alpha = 61.9^\circ$)

View number	-4	-3	-2	-1	0	1	2	3	4
x_2 (pixel)	-312	-234	-156	-78	0	78	156	234	312
x_1 (pixel)+	-269	-199	-132	-65	0	65	132	199	269
x_1 (pixel)*	-175	-131	-87	-43	0	43	87	131	175
α_{21} (degrees)+	-5.703	-4.255	-2.827	-1.410	0.000	1.410	2.827	4.255	5.703
α_{21} (degrees)*	-0.010	-0.008	-0.005	-0.003	0.000	0.003	0.005	0.008	0.010
r (mm)	56.489	42.732	28.666	14.387	0.000	14.387	28.666	42.732	56.489

Note: + means before adjustment, * means after adjustment

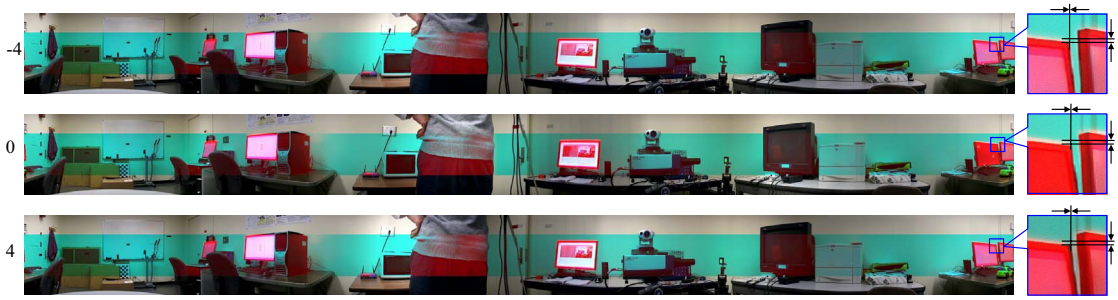

(a) Before adjustment

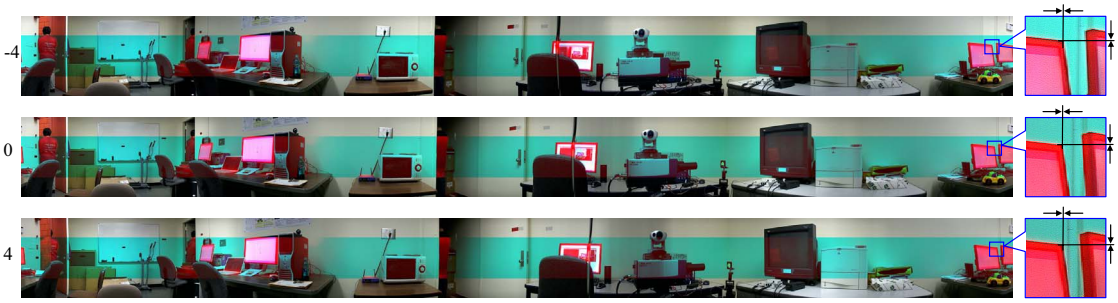

(b) After adjustment

Fig. 8. Alignment results of EO and IR image

[7] W. Jiang, M. Okutomi, and S. Sugimoto, "Panoramic 3d reconstruction using rotational stereo camera with simple epipolar constraints," *IEEE Conf. CVPR*, pp. 947–953, 2006.

[8] Y. Li, H. Shum, C. Tang, and R. Szeliski, "Stereo reconstruction from multiperspective panoramas," *IEEE Trans. PAMI*, vol. 26, pp. 45–62, 2004.

[9] P. Peer and F. Solina, *Multiperspective panoramic depth imaging*, ser. Computer Vision and Robotics, J. X. Liu, Ed. New York: Nova Science, 2006.

[10] S. Peleg, M. Ben-Ezra, and Y. Pritch, "Omnistereo: panoramic stereo imaging," *IEEE Trans. PAMI*, vol. 23, pp. 279–290, 2001.

[11] S. Tzavidas and A. K. Katsaggelos, "A multicamera setup for generating stereo panoramic video," *IEEE Trans. on Multimedia*, vol. 7, pp. 880–889, 2005.

[12] J. Zheng and S. Tsuji, "Panoramic representation for route recognition by a mobile robot," *IJCV*, vol. 9, pp. 55–76, 1992.

[13] Z. Zhu, E. M. Riseman, and A. R. Hanson, "Generalized parallel-perspective stereo mosaics from airborne videos," *IEEE Trans. PAMI*, vol. 26, pp. 226–237, 2004.

[14] H. Chang, A. Koschan, M. ABidi, S. G. Kong, and C. Won, "Multi-spectral visible and infrared imaging for face recognition," *IEEE Conf. CVPR*, pp. 1–6, 2008.

[15] N. Cvejic, J. Lewis, D. Bull, and N. Canagarajah, "Adaptive region-based multimodal image fusion using ICA bases," *Int. Conf. Information Fusion*, pp. 1–6, 2006.

[16] M. Hild and G. Umeda, "Image registration in stereo-based multi-modal imaging systems," *Int. Symp. Image and Signal Processing and Analysis*, pp. 70–75, 2005.

[17] D. A. Socolinsky, *Design and deployment of visible-thermal biometric surveillance systems*, ser. Multimodal Surveillance: Sensors, Algorithms and Systems, Z. Zhu and T. S. Huang, Eds. Norwood: Artech House, 2007.

[18] A. Zomet and S. Peleg, "Multi-sensor super-resolution," *IEEE Workshop on Applications of Computer Vision*, pp. 27–31, 2002.

[19] R. C. Bolles, H. H. Baker, and D. H. Marimont, "Epipolar-plane image analysis: an approach to determining structure from motion," *Int. J. Computer Vision*, vol. 1, pp. 7–55, 1987.

[20] E. Molina, Y. Qu, W. L. Khoo, and Z. Zhu, "Mosaic based multimodal, multi-view and stereo rendering," http://visionlab.engr.ccny.cuny.edu/~molina/publications/ccny_mm3p.mov.